Progress In Electromagnetics Research Letters, Vol. 81, 113–120, 2019

CPW-Fed Dual-Band Dual-Sense Circularly Polarized Antenna for WiMAX Application

Manas Midya*, Shankar Bhattacharjee, and Monojit Mitra

Abstract—This paper presents a CPW-fed dual-band dual-sense circularly polarized square slot antenna (CPSSA). The antenna consists of a rectangular radiator with two unequal rectangular strips, connected by a CPW feed line. An inverted L-shaped grounded stub is placed in the right side of the slotted ground plane with the orthogonal direction of the feed line to create CP modes. The proposed antenna obtained two CP bandwidths of 3.30–3.78 GHz and 5.4–5.86 GHz with axial ratio (AR) value less than 3 dB, and both the CP bands are overlapped by impedance bandwidth (IBW) of the antenna, ranging from 2.72 to 7.34 GHz. Total size of the proposed antenna is $50 \times 50 \times 1.58$ mm^3. The antenna is fabricated on an FR4-epoxy substrate and measured. Simulation results are verified by measurement for the given antenna. The designed antenna is well used for WiMAX (3.5 GHz and 5.5 GHz) band with CP characteristics. Design procedures of the antenna are discussed in details for further understanding of the antenna design. Parametric study has been done for describing the mechanism of the dual-band CP with the analysis of electric current distribution of the antenna. Meanwhile, wide axial ratio bandwidth has been obtained in both the bands using this structure compared to other published structures.

1. INTRODUCTION

With the increasing demand of circularly polarized antennas for multipurpose applications, multiband CP antenna design takes the attention of worldwide researchers. CP antenna has distinct advantages over linearly polarized antenna, such as minimum polarization mismatch and multipath interference, better mobility and better weather penetration power [1]. For CP wave generation, two orthogonal electric fields of equal amplitude with 90° phase difference are required [2]. Different types of structure have been proposed in open literature for generating CP waves. Among them, CPW-fed slot antenna is one of the advantageous techniques (low profile and easy fabrication) to realize CP performance. However, limitation of AR bandwidth is the immense drawback, which leads to the restriction of broadband CP antenna applications. Multiband CP antenna can be realized by rotating two rectangular patches [3], placing a T-shaped stub with two spiral slots or an asymmetric feed line in a square slot ground plane [4–6], implementing a crane-shaped grounded stub with two parallel monopoles or a C-shaped grounded strip with slots loaded in a square slot ground plane [7, 8], stacking two different corner truncated patches [9], exciting a spiral, annular ring slot or two circular eccentric rings [10–13], implementing four T-shaped elements or slits into the edge of the square slot [14], perturbing the patch with modified ground plane [15, 16], using a tilted-D shaped or grounded stub loaded monopole antenna [17–19]. However, design of wider ARBW for a dual-band dual-sense CP antenna is still a big challenge for researchers.

Here we propose a dual-band dual-sense CP antenna with wide AR bandwidth for WiMAX application. Two unequal rectangular strips are connected with the rectangular patch, and an inverted

Received 13 September 2018, Accepted 28 November 2018, Scheduled 30 January 2019

* Corresponding author: Manas Midya (letsmanas@gmail.com).

The authors are with the Department of Electronics & Telecommunication Engineering, Indian Institute of Engineering Science & Technology, Shibpur, India.

L-shaped grounded stub is orthogonally placed in the square slot ground plane to realize the dual wideband CP antenna. The CP bandwidth of the proposed antenna, ranging from 3.30 to 3.78 GHz (13.56%) and 5.40 to 5.86 GHz (8.17%), covers the WiMAX band. Impedance bandwidth of the proposed antenna is 91.85% (2.72–7.34 GHz) which overlaps with the CP bands of the proposed antenna.

2. ANTENNA DESIGN AND ANALYSIS

Figure 1 shows the geometry of the proposed antenna which is etched on a 1.58 mm thick economic FR4-epoxy substrate ($\varepsilon_r = 4.4$ and $\tan\delta = 0.02$). Initially a square slot ($32 \times 32\,\text{mm}^2$) is etched on the top of the substrate, and a rectangular metal radiator is placed into the square slot. To excite this rectangular metal strip, a 3 mm wide and 11.2 mm long CPW-feed line is chosen with 0.3 mm gap from both sides of the ground plane, shown in Fig. 2 (Ant. 1). After that, a rectangular strip with larger length (l_1) is placed at left side of the radiating edge of initially placed rectangular strip in Ant. 2. In the very next step, another rectangular strip with shorter length (l_2) is connected to the radiating edge (right side) of the rectangular strip (Ant. 3). With the inclusion of these two strips, the square slot antenna starts radiating at two different frequencies with linearly polarized wave in broadside direction. In Ant. 4, an inverted-L shaped grounded strip is placed into the right side of the slotted ground plane in orthogonal direction of the CPW feed line. Grounded stub is preferred to be placed in the right side of the slotted ground plane because of the existence of larger magnetic current distribution at the right half of the square slot. Due to the inclusion of grounded stub, fundamental modes of the antenna are split into two near-degenerative orthogonal modes with equal amplitude and 90° phase difference, which is responsible for CP radiation of the antenna at two distinct frequencies. After the parametric study on the length of the rectangular strips and inverted-L shaped stub, final values are chosen for

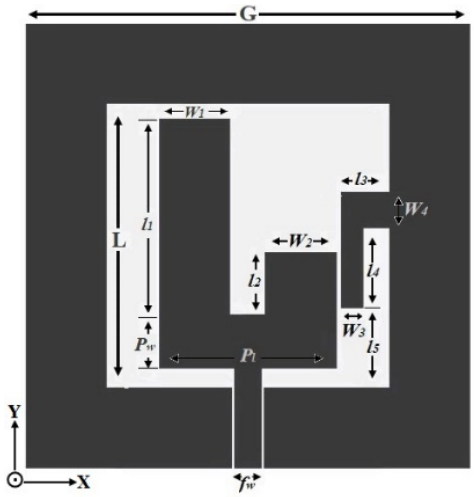

Figure 1. Top view of the designed antenna. ($G = 50$, $L = 32$, $f_w = 3$, $P_w = 6$, $P_l = 20$, $l_1 = 22$, $W_1 = 8$, $l_2 = 7$, $W_2 = 8$, $l_3 = 5.5$, $l_4 = 9$, $l_5 = 9$, $W_3 = 2.5$, $W_4 = 4$) (unit: millimeters).

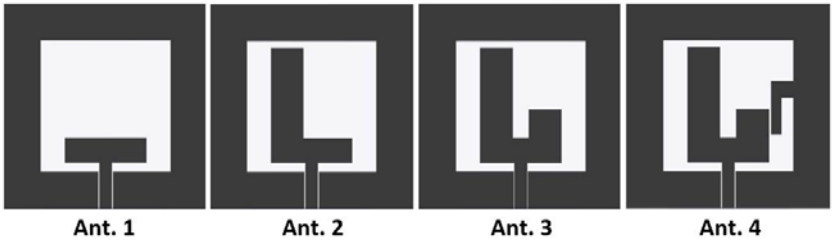

Figure 2. Evaluation of the design.

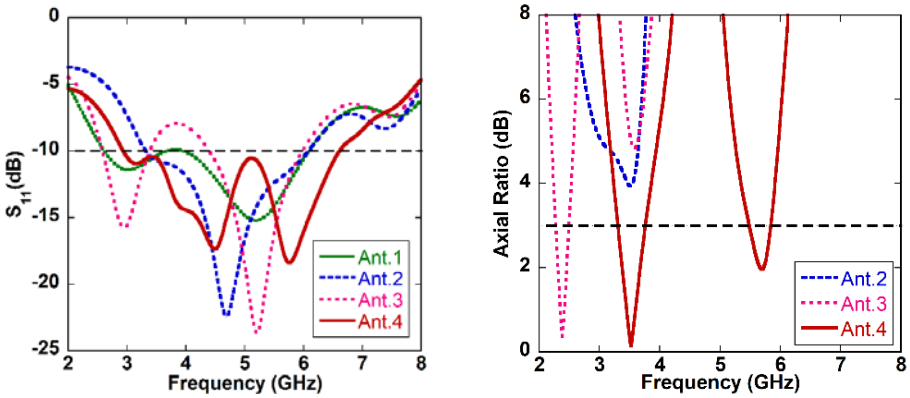

(a) (b)

Figure 3. Simulated results for different evaluation steps of the antenna (a) S_{11}, (b) axial ratio.

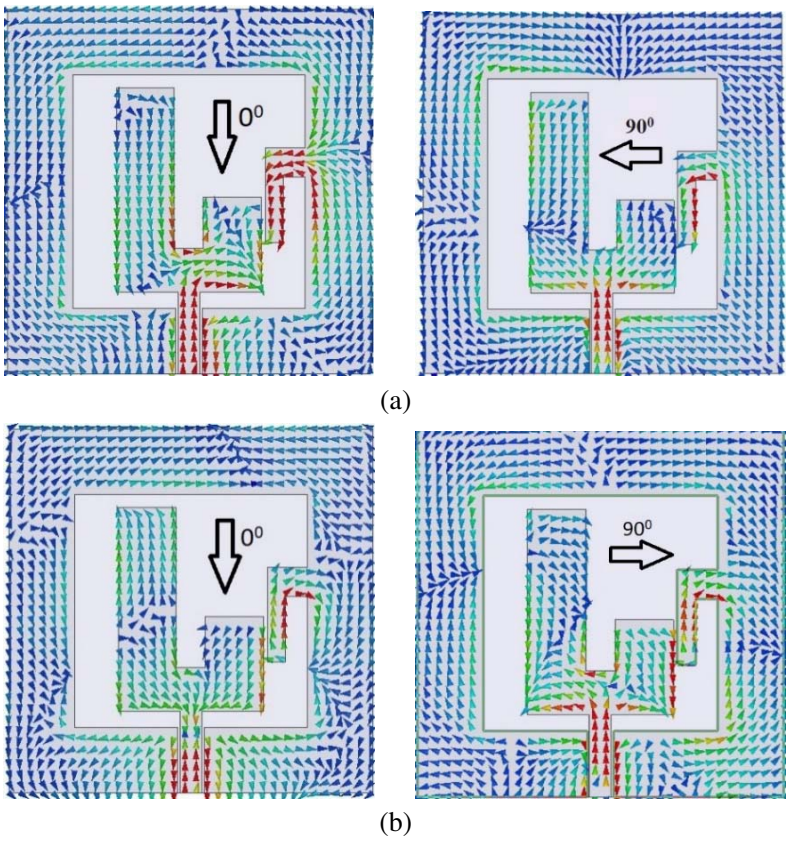

(a)

(b)

Figure 4. Surface current distribution of the antenna (a) at 3.5 GHz, (b) at 5.7 GHz.

generating two wide ARBWs (3.30–3.78 GHz and 5.40–5.86 GHz) within the IBW (2.72–7.34 GHz) of the antenna. Figs. 3(a) & (b) show the return loss and axial ratio plots of the antenna improvement steps (Ant. 1–4). Here the proposed antenna provides the left-hand CP (LHCP) and right-hand CP (RHCP) for the lower and upper bands, respectively. As we can see, lower resonant mode of the antenna comes due to the longer strip of the antenna, and the direction of surface current rotation is clockwise against time, shown in Fig. 4(a). So, LHCP would be achieved for the lower band. On the other hand, upper resonant mode is achieved by the shorter arm of the antenna, and the rotation of surface current is counter-clockwise, which leads to RHCP at the upper band, shown in Fig. 4(b).

Table 1. Comparison with reported dual-band dual-sense CP antennas.

Ref.	Size (mm^3)	Impedance BW (%)	Axial Ratio BW (%)	Sense of Polarization
[10]	100×100×1.57	18.2%, 18.4%	4.45%, 3.5%	RHCP, LHCP
[11]	95×80×1.6	25.6%, 20%	5.6%, 2.4%	LHCP, RHCP
[12]	66×55×1.6	22.7%, 22.3%	3.6%, 5.6%	LHCP, RHCP
[14]	70×70×3.0	1.8%, 2.6%	0.4%, 0.6%	RHCP, LHCP
Proposed	50×50×1.58	91.85%	13.56%, 8.17%	LHCP, RHCP

Comparisons between the proposed antenna and previous antennas are shown in Table 1 which includes antenna size, IBW, 3 dB ARBW, and sense of polarization. It interprets that the proposed antenna has the superiority of compact size and widest ARBW with a quite simple structure.

Different key parameters are studied in the next section to analyse their effects on antenna performance. The lengths of two different size strips (l_1, l_2) and grounded stub length have great influence on IBW and ARBW of the antenna. In order to give the organized description and find the relationship between key parameters, IBW and ARBW, a wide parametric study has been done using finite element method-based solver ANSYS high-frequency structure simulator (HFSS-13). Three parameters are chosen here for parametric analysis. Other parameters are kept constant at their final values at the time of parametric study of one parameter. The next section provides details about different parameters which are considered during parametric analysis of the designed antenna.

2.1. Effect of Longer Rectangular Strip Length (l_1)

The length of the longer rectangular strip (l_1) connected to the patch is varied step wise in this analysis. From Figs. 5(a) & (b), it can be inferred that lower cutoff frequency is shifted left and overlapped with the lower ARBW of the antenna when the length of the strip (l_1) is increased. From Fig. 5, we observe that impedance matching and axial ratio of the lower band are highly affected by larger strip length variation. The higher resonating frequency and ARBW shifts left, but in this case the rate of change is small. At $l_1 = 22$ mm maximum ARBW is obtained for the designed antenna.

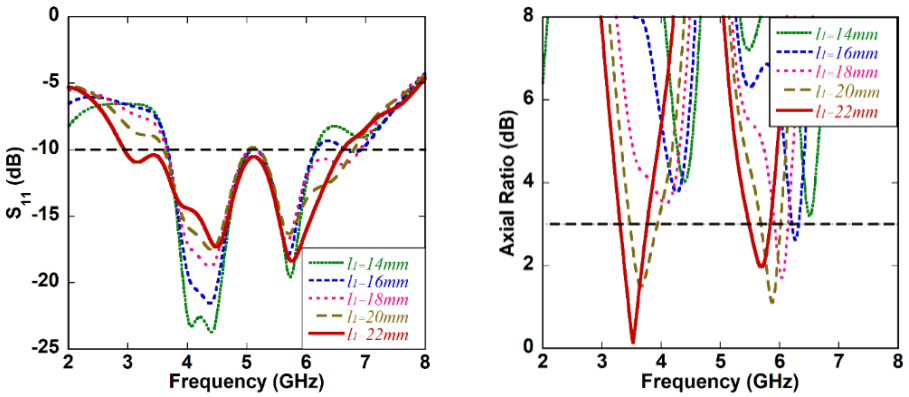

(a) (b)

Figure 5. Simulated results for different value of left-strip length (a) S_{11}, (b) axial ratio.

2.2. Effect of Shorter Rectangular Strip Length (l_2)

The case study of shorter rectangular strip length (l_2) variation is performed for S_{11} and axial ratio values. The results of the analysis are shown in Figs. 6(a) & (b). Increasing the length of the smaller strip increases the electric current path length, thereby the resonant frequency of higher band shifts left whereas the resonating frequency of the lower band is less affected as shown in Fig. 6(a). The ARBW of the higher band is more sensitive with right-strip length (l_2) variation over the lower band. Thus, increasing the strip length improves the ARBW of the higher band more effectively over the lower band. Finally, l_2 is chosen as 7 mm for obtaining better CP performance of the antenna.

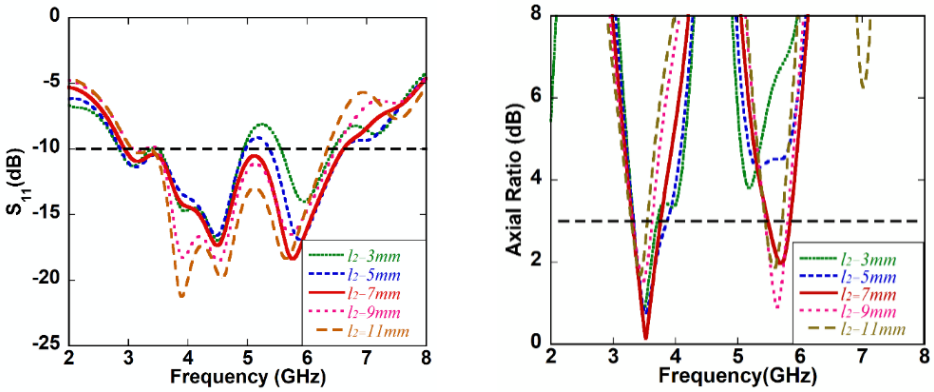

Figure 6. Simulated results for different value of right-strip length (a) S_{11}, (b) axial ratio.

2.3. Effect of Stub Length (l_4)

The effect of stub length is studied in this analysis. During the simulations, the left-strip length (l_1) and right-strip length (l_2) are kept unvaried. The results are shown in Figs. 7(a) & (b). The grounded stub length has a significant effect on IBW as well as ARBW of the proposed antenna. It can be observed that the increase of stub length improves the impedance matching of the antenna, and ARBW of the higher band is more affected over the lower ARBW. Considering the desired frequency range (simulated) from 2.9 to 6.60 GHz, the finest length can be chosen as 9 mm where the two curves intersect as shown in Figs. 7(a) & (b).

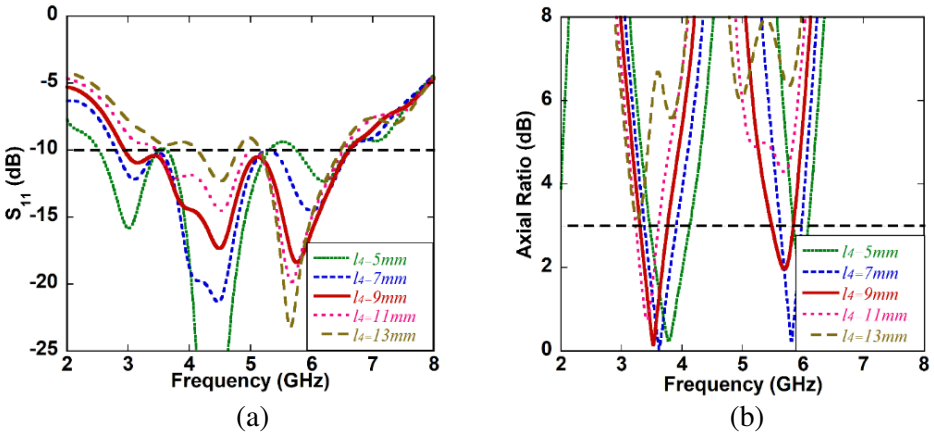

Figure 7. Simulated results for different value of stub length (a) S_{11}, (b) axial ratio.

3. EXPERIMENTAL RESULTS AND DISCUSSION

On the basis of the parametric analysis, the optimized dimensions of the antenna are obtained, and the antenna prototype is fabricated. The optimized dimensions of the antenna are shown in Fig. 1. The antenna has overall dimensions of $50 \times 50 \times 1.58\,\text{mm}^3$. Initially the antenna is designed for dual-band application with linear polarization (LP), as shown in Fig. 2 (Ant. 3). However, when the grounded stub is placed in the square slot (Ant. 4), the fundamental modes of the antenna split into two near-degenerative orthogonal modes with equal amplitude and 90° phase difference for CP operation in two bands. The fabricated antenna is shown in Fig. 8(a). The S_{11} parameters of the fabricated antenna are measured using Anritsu vector network analyser. The measured S_{11} result covers the frequency range of 2.72–7.34 GHz effectively as shown in Fig. 8(b). The measured ARBW bandwidth ranges from 3.30 to 3.78 GHz for the lower band whereas for the higher band it is from 5.40 to 5.86 GHz. A little mismatch of S_{11} parameters is due to the fabrication tolerance on account of the manual soldering process. Maximum measured gains of the antenna are 3.03 dB and 3.42 dB in the lower and upper bands, respectively, shown in Fig. 9(a). The efficiency of the antenna is measured using Wheeler cap method, and results are shown in Fig. 9(b).

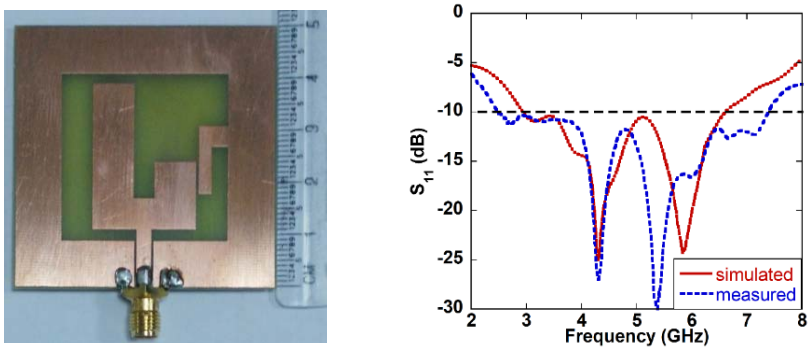

(a) (b)

Figure 8. (a) Prototype of the designed antenna and (b) simulated and measured S_{11}.

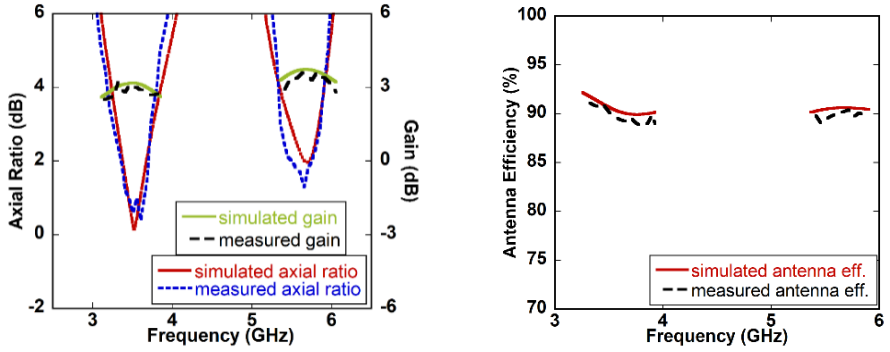

(a) (b)

Figure 9. Simulated and measured results (a) axial ratio and gain, (b) antenna efficiency.

Simulated and measured normalized LHCP and RHCP radiation patterns of the proposed antenna are shown in Fig. 10(a) at 3.5 GHz and Fig. 10(b) at 5.7 GHz. As the antenna has bidirectional property, it shows that at 3.5 GHz the antenna radiates LHCP wave in the boresight direction ($Z > 0$) and RHCP wave in the opposite direction of positive Z-direction ($Z < 0$). On the other hand, at 5.7 GHz, the proposed antenna radiates RHCP wave in the upper side ($Z > 0$) of the ground plane and LHCP wave in the opposite side ($Z < 0$) of the ground plane. The range of angles around broadside over which AR is less than 3 dB is given in Table 2.

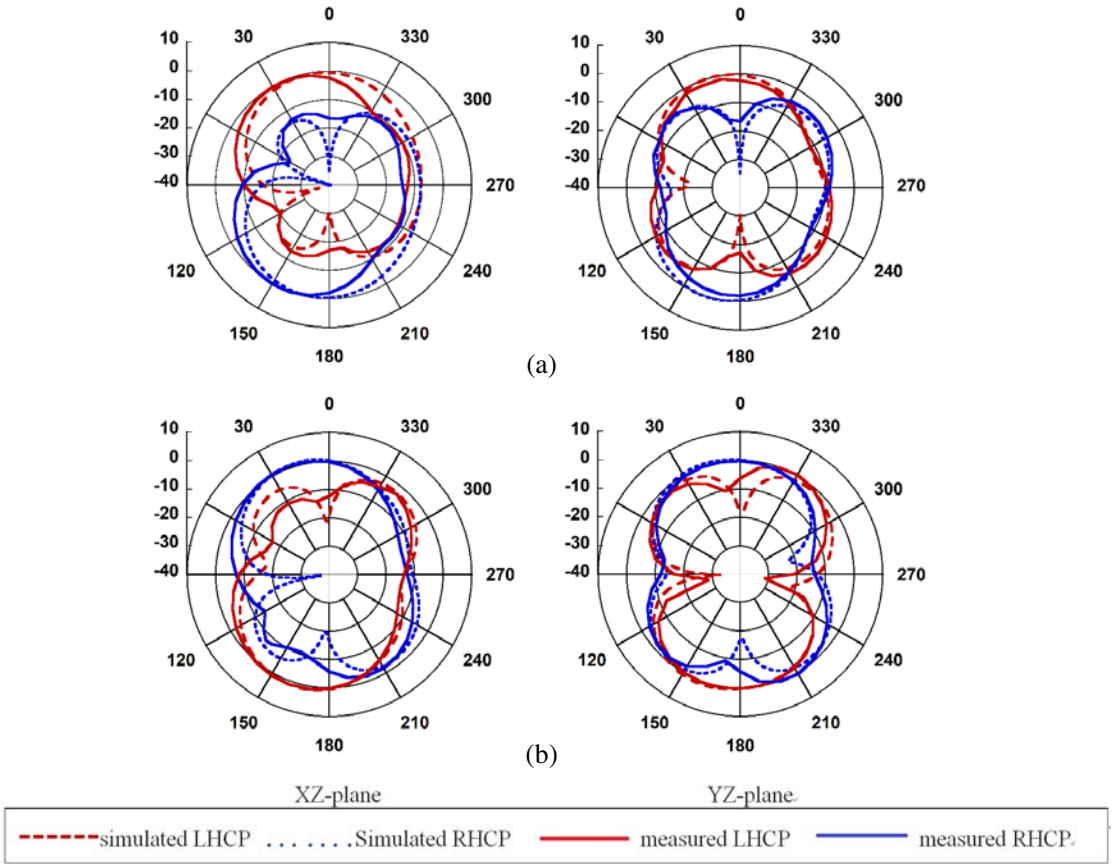

Figure 10. Simulated and measured normalized radiation patterns: (a) 3.5 GHz, (b) 5.7 GHz.

Table 2. The range of angles around broadside where AR $\leq$ 3 dB.

Frequency (GHz)	3.3	3.4	3.5	3.6	3.7
XZ-plane	$\theta=12^0$	$\theta=32^0$	$\theta=34^0$	$\theta=31^0$	$\theta=19^0$
YZ-plane	$\theta=14^0$	$\theta=21^0$	$\theta=18^0$	$\theta=13^0$	$\theta=10^0$
Frequency (GHz)	5.4	5.5	5.6	5.7	5.8
XZ-plane	$\theta=8^0$	$\theta=10^0$	$\theta=14^0$	$\theta=17^0$	$\theta=10^0$
YZ-plane	$\theta=14^0$	$\theta=11^0$	$\theta=10^0$	$\theta=8^0$	$\theta=6^0$

4. CONCLUSION

A CPW-fed dual-band dual-sense CP antenna with wide ARBW is proposed here. Two different sized strips with an inverted-L grounded stub are used to obtain dual-band dual-sense CP. The designed antenna covers the WiMAX (3.5 GHz and 5.5 GHz) bands efficiently with maximum gains of 3.03 dB and 3.42 dB in lower and upper CP bands, respectively. The measured IBW of the proposed antenna is 4.62 GHz (91.85%, 2.72–7.34 GHz) and ARBWs are 0.48 GHz (13.56%, 3.30–3.78 GHz) and 0.46 GHz (8.17%, 5.40–5.86 GHz) in the lower and upper bands, respectively. Considering its simple structure, light weight, low cost and dual-band dual-sense property, the antenna is found to be a potential candidate for modernday wireless applications.

REFERENCES

1. Gao, S., Q. Luo, and F. Zhu, *Circularly Polarized Antennas*, John Willey and Sons, West Sussex, UK, 2014.
2. Kumar, G. and K. P. Ray, *Broad Band Microstrip Antennas*, Artech House, Boston, MA, 2003.
3. Liu, A. X., L. Chen, X. J. Zhong, H. Wang, and X. W. Shi, "A novel design of dual-band circularly polarized antenna based on patches having rotation angles," *Progress In Electromagnetics Research Letters*, Vol. 54, 107–113, 2015.
4. Chen, C. and E. K. N. Yung, "Dual-band dual-sense circularly-polarized CPW-fed slot antenna with two spiral slots loaded," *IEEE Transactions on Antennas and Propagation*, Vol. 57, No. 6, 1829–1833, 2009.
5. Saini, R. K. and S. Dwari, "Dual-band dual-sense circularly polarized square slot antenna with changeable polarization," *Microw. Opt. Technol. Lett.*, Vol. 59, 902–907, 2017.
6. Rui, X., J. Li, and K. Wei, "Dual-band dual-sense circularly polarized square slot antenna with simple structure," *Electron. Lett.*, Vol. 52, No. 8, 578–580, 2016.
7. Chen, C. H. and E. K. N. Yung, "Dual-band circularly-polarized CPW-fed slot antenna with a small frequency ratio and wide bandwidths," *IEEE Transactions on Antennas and Propagation*, Vol. 59, No. 4, 1379–1384, 2011.
8. Chen, Y. Y., Y. C. Jiao, G. Zhao, F. Zhang, Z. L. Liao, and Y. Tian, "Dual-band dual-sense circularly polarized slot antenna with a c-shaped grounded strip," *IEEE Antennas and Wireless Propagation Letters*, Vol. 10, 915–918, 2011.
9. Ooi, T. S., S. K. A. Rahim, and B. P. Koh, "2.45 GHz and 5.8 GHz compact dual-band circularly polarized patch antenna," *Journal of Electromagnetic Waves and Applications*, Vol. 24, 1473–1482, 2010.
10. Bao, X. L. and M. J. Ammann, "Monofilar spiral slot antenna for dual-frequency dual-sense circular polarization," *IEEE Transactions on Antennas and Propagation*, Vol. 59, No. 8, 3061–3065, 2011.
11. Lei, Z. Y., J. W. Zhang, R. Yang, X. Liu, L. Chen, and X. H. Kong, "Design of dual-band dual-sense circularly polarized slot antenna," *Progress In Electromagnetics Research C*, Vol. 43, 41–51, 2013.
12. Wang, C., J. Li, W. T. Joines, and Q. H. Liu, "Dual-band capacitively loaded annular-ring slot antenna for dual-sense circular polarization," *Journal of Electromagnetic Waves and Applications*, Vol. 31, 867–878, 2017.
13. Yang, K. P. and K. L. Wong, "Dual-band circularly-polarized square microstrip antenna," *IEEE Transactions on Antennas and Propagation*, Vol. 49, No. 3, 377–382, 2001.
14. Liang, Z. X., D. C. Yang, X. C. Wei, and E. P. Li, "Dual-band dual circularly polarized microstrip antenna with two eccentric rings and an arc-shaped conducting strip," *IEEE Antennas and Wireless Propagation Letters*, Vol. 15, 834–837, 2016.
15. Chang, T. N. and J. M. Lin,"Dual-band circularly polarized monopole antenna," *Journal of Electromagnetic Waves and Applications*, Vol. 29, 843–857, 2015.
16. Chen, B. and F. S. Zhang, "Dual-band dual-sense circularly polarized slot antenna with an open-slot and a vertical stub," *Progress In Electromagnetics Research Letters*, Vol. 48, 51–57, 2014.
17. Altaf, A. and M. Seo, "A tilted-D-shaped monopole antenna with wide dual-band dual-sense circular polarization," *IEEE Antennas and Wireless Propagation Letters*, DOI: 10.1109/LAWP.2018.2878334.
18. Lu, J. H. and C. W. Liou, "Planar dual-band circular polarization monopole antenna for wireless local area networks," *IEEE Antennas and Wireless Propagation Letters*, Vol. 14, 478–481, 2015.
19. Saini, R. K., S. Dwari, and M. K. Mandal, "CPW-fed dual-band dual-sense circularly polarized monopole antenna," *IEEE Antennas and Wireless Propagation Letters*, Vol. 16, 2497–2500, 2017.